Materials Today Physics 12 (2020) 100191

Contents lists available at ScienceDirect

Materials Today Physics

journal homepage: https://www.journals.elsevier.com/materials-today-physics

Epidermal electrodes with enhanced breathability and high sensing performance

Y. Wang [a, e], T. Hong [a, e], L. Wang [a], G. Li [a], N. Bai [a], C. Li [a], P. Lu [a], M. Cai [a], Z. Wu [a, b], N. Lu [c], B. Yu [d], J. Zhang [a, **], C.F. Guo [a, *]

[a] Department of Materials Science & Engineering, And Centers for Mechanical Engineering Research and Education at MIT and SUSTech, Southern University of Science and Technology, Shenzhen, 518055, China
[b] State Key Laboratory of Digital Manufacturing Equipment and Technology, Huazhong University of Science and Technology, Wuhan, 430074, China
[c] Department of Aerospace Engineering and Engineering Mechanics, University of Texas at Austin, Austin, TX, 78712, USA
[d] Ningbo Fengcheng Advanced Energy Materials Research Institute, Fenghua District, Ningbo, Zhejiang, 315500, China

ARTICLE INFO

Article history:
Received 17 January 2020
Received in revised form
5 February 2020
Accepted 5 February 2020
Available online 20 February 2020

Keywords:
Conformable contact
Strain sensing
Nanomesh
Wettability
Cold welding

ABSTRACT

High breathability of epidermal electronics plays a critical role in long-term attachment and non-irritating contact to the skin. However, most existing skin-mounted electronics use a water-proof substrate (*e.g.*, 3M Tegaderm), which hinders skin sweating, resulting in interfacial delamination and skin irritation. Here, we report that hydrophilically treated Au nanomeshes (AuNMs) exhibit a sweat evaporation rate significantly faster than that of naked skin while maintaining high stretchability and exceptional conformability. The epidermal AuNM is able to stably sense body motions and detect the strain level of the skin as well as joint bending directions. The sensing capability results from local rupture and fast cold welding of Au nanowires during deformation, which contributes to fast healing or repair of damaged AuNM epidermal circuits. Such substrate-free AuNMs with improved breathability are promising for high performance on skin electronics and beyond.

1. Introduction

Skin-like electronics is an emerging field aimed at merging flexible electronic devices with the human body or soft robots. The rapid development of the new field calls for materials and devices with high stability and high fidelity in measuring physical, chemical, and physiological signals of the human body [1–7], while maintaining long-term conformal contact with the contours of human skin during usage [8,9]. Extensive contributions have been made to meet those demands [10–14]. For human body applications, sweat breathability of on-skin electronics has been a major consideration for comfortable wearing and long-term conformal contact to the skin, to avoid detachment and irritation to human skin. However, existing electronic assemblies typically consist of blanket membranes or multilayers (*e.g.*, by using an elastomeric substrate and a few layers of active materials) [13,15–19]. Such structures strongly limit their sweat breathability and the conformability to skin textures. Although some breathable elastomeric materials [20–22] and substrate-free metal networks [23] have been developed to solve the problem, skin with such materials still exhibits poorer sweat breathability than naked skin. The discomfort resulted from perspiration especially that caused by strenuous exercises or relatively high temperatures has thus become a big concern.

Although the mesh structure allows for high flexibility and high gas permeability, small thickness of the mesh is critical to achieve high conformability. Here, we show that a substrate-free Au nanomesh (AuNM) with a thickness of only 30 nm made by grain boundary lithography exhibits high stretchability and full conformability to human skin textures. When a monolayer of 1-thioglycerol molecules is assembled onto the AuNM, the AuNM-covered skin exhibits dramatically improved hydrophilicity that allows sweat droplets to fully wet the skin. The improved hydrophilicity of the AuNM-covered skin significantly boosts the sweat evaporation rate with a factor of ~3.6 in reference to naked skin. On the other hand, the AuNM can be used as an on-skin strain sensor

* Corresponding author.
** Corresponding author.
E-mail addresses: zhangjm@sustech.edu.cn (J. Zhang), guocf@sustech.edu.cn (C.F. Guo).
[e] These authors contributed equally to this work.

https://doi.org/10.1016/j.mtphys.2020.100191
2542-5293/

that is capable of sensing human motion such as finger bending and wrist rotation with high-fidelity signals. The sensing capability lies in the delocalized rupture of the AuNM upon stretching and fast cold welding of Au nanowires upon releasing. Such a cold welding mechanism also enables fast reconnection or healing of damaged AuNM circuits with an overlay alignment. A highly stretchable and conformable on-skin thermotherapy with a fast heating rate and precise temperature controllability has been demonstrated. Such an AuNM is an ideal selection as a comfortable and long-term attachable electrode for epidermal electronics and may also be used to build other conformable devices other than on-skin electronics.

2. Results and discussion

2.1. Transfer and conformability of the AuNM on skin

The AuNM was made by grain boundary lithography, and it floated on water before transfer [24]. A large area of the non-patterned AuNM was then transferred to human skin, followed by blowing with a stable and directional airflow to remove the water between the AuNM and skin (Fig. 1a). Next, a mask of scotch tape with the desired pattern was attached to the epidermal AuNM, and the unnecessary part was peeled off, leaving behind the designed pattern (Fig. S1). After testing, the AuNM can be easily removed by washing with water owing to the poor adhesion to human skin. For demonstration, a patterned AuNM with the shape of the southern university of science and technology (SUSTech) badge was made and attached on the skin, which was found to comply well with the skin texture. The AuNM on skin is exceptionally flexible and can be significantly stretched or squeezed on skin without being delaminated, behaving like a tattoo (Fig. 1b and S2). The AuNM also exhibits a high transmittance of 83.6% (Fig. 1c and S3) that may enable applications in some medical and optical purposes.

The aforementioned properties of the AuNM are highly correlated to its microstructure. First, the mesh consists of serpentine ligaments with a line width of tens of nanometers, as shown in the scanning electron microscopy (SEM) image of Fig. 1d. It has been proven that both serpentines and networks are effective to achieve high stretchability [25,26]. Second, the nanoscale thickness (~30 nm) is critical to high conformability. The SEM image (Fig. 1d) shows an AuNM that complies well with the texture of a piece of dead skin. The high conformability of the AuNM on a soft substrate, *e.g.*, human skin, is predicted by the energy minimization method which was proposed by Wang et al. [14] and Wang and Lu [27]. The total energy U_{total} of the film-skin system can be written as follows:

$$U_{total} = U_{bending} + U_{adhesion} + U_{skin} \tag{1}$$

where $U_{bending}$ is the bending energy of the film, $U_{adhesion}$ is the interface adhesion energy between the film and the human skin, and U_{skin} is the elastic energy stored in the deformed skin. Detailed information on the terms in Equation (1) can be found in the Supporting Information Appendix. In general, the degree of conformability can be characterized as the ratio between the contact zone (x_c) and the total area ($\lambda_0/2$)). As depicted in Appendix figure, it is defined as $\widehat{x}_c = \frac{2x_c}{\lambda_0}$. A fully conformed scenario means $\widehat{x}_c = 1$ is achieved. As explained in supplementary theory, for an electrode-skin system with the given parameters, i.e., λ_0, h_0, t, $\overline{E}_m$, $\overline{E}_s$, γ (where λ_0 and h_0 represent the wavelength and amplitude of the undeformed skin, respectively, t represents the thickness of AuNM, $\overline{E}_m$ represents the plane strain modulus of Au, $\overline{E}_s$ represents the plane strain modulus of human skin, and γ represents the adhesion between Au and human skin [the detailed values of which are listed in Table 1]), minimization of the total energy of the system U_{total} with respect to h_1 (the new amplitude) and x_c yields the equilibrium state.

Note that for the AuNM, the effective bending rigidity is simply treated as follows:

$$\overline{EI}_{mesh} = \rho \overline{EI}_{Au} \tag{2}$$

where $\rho = 29.7\%$ is the area fraction of Au in the nanomesh as per SEM observation.

Our calculation shows that the critical thickness of the AuNM to be fully conformed is ~87 nm. In other words, our AuNM with a ~30-nm thickness, which is much thinner than this critical value, will achieve conformal contact to the skin. The specific relationship between conformability and AuNM thickness is shown in Fig. 1e.

2.2. Breathability and compatibility of the AuNM

Sweat breathability is a crucial property to comfortable wearing and long-term usage of epidermal electronics. Poor breathability, on the one hand, may cause electrochemical corrosion to electronic materials and skin irritation; and on the other hand, it may impair the attachment of electronic materials because of the trapped moisture at the device-skin interface (Fig. S4) [21,22]. Here, for the substrate-free AuNM, both sweat and water vapor can freely penetrate through the nanoscale mesh (Fig. 2a). We have experimentally observed that the AuNM has almost no hindrance to gas permeability (Fig. S5) by comparing the weight losses of water penetrating through a gas-permeable membrane and through a counterpart covered by an AuNM.

Wettability plays an important role in sweat breathability; therefore, it is possible to improve the sweat evaporation rate of the skin by enhancing the wettability of the epidermal AuNM. Typically, the water contact angle of the naked skin is ~75°, which is not low enough for fast evaporation of sweat. Although Au is a hydrophilic material such that an epidermal AuNM can slightly improve the wettability of skin, the effect is quite limited because of the small area fraction of Au. To significantly improve the sweat evaporation rate, a monolayer of 1-thioglycerol molecules was introduced onto the AuNM surface (Fig. 2b), and this hydrophilic treatment was found to remarkably decrease the water contact angle to about 10° (Fig. 2c) which allows sweat droplets to spread dramatically. As a result, the AuNM-covered skin exhibits a higher sweat evaporation rate than that of naked skin (see Movie S1 and Fig. 2d), and statistical data indicate that the hydrophilically treated AuNM will improve the sweat evaporation rate of skin with a factor higher than 3. In our experiment, the average sweat evaporation time toward drying for the naked skin is 13.7 s. By contrast, for the skin covered by the hydrophilically treated AuNM, the period of time toward drying decreases to 3.7 s (Fig. 2e) and that for the skin with the untreated AuNM is ~6.3 s (Fig. S6). The hydrophilic treatment is proven to be quite effective in improving the sweat evaporation rate. The AuNM, on the other hand, has little influence on sweat secretion (see Movie S2, which shows that sweat secretion behaviors for the naked skin and the AuNM-covered skin are similar) because of the low flow rate of sweat and hydrophilic nature of the mesh.

Supplementary video related to this article can be found at https://doi.org/10.1016/j.mtphys.2020.100191.

Theoretically, for a droplet, the mass-loss rate is proportional to its surface area [31,32]; therefore, skin surface with a lower water contact angle will allow the sweat droplet to fully wet the skin and thus accelerate sweat evaporation. During evaporation, the droplet thickness reduces, but the area remains almost constant (which is evidenced by the formation of the coffee ring), and as a result, the evaporation rate also remains approximately constant [33,34]. For a

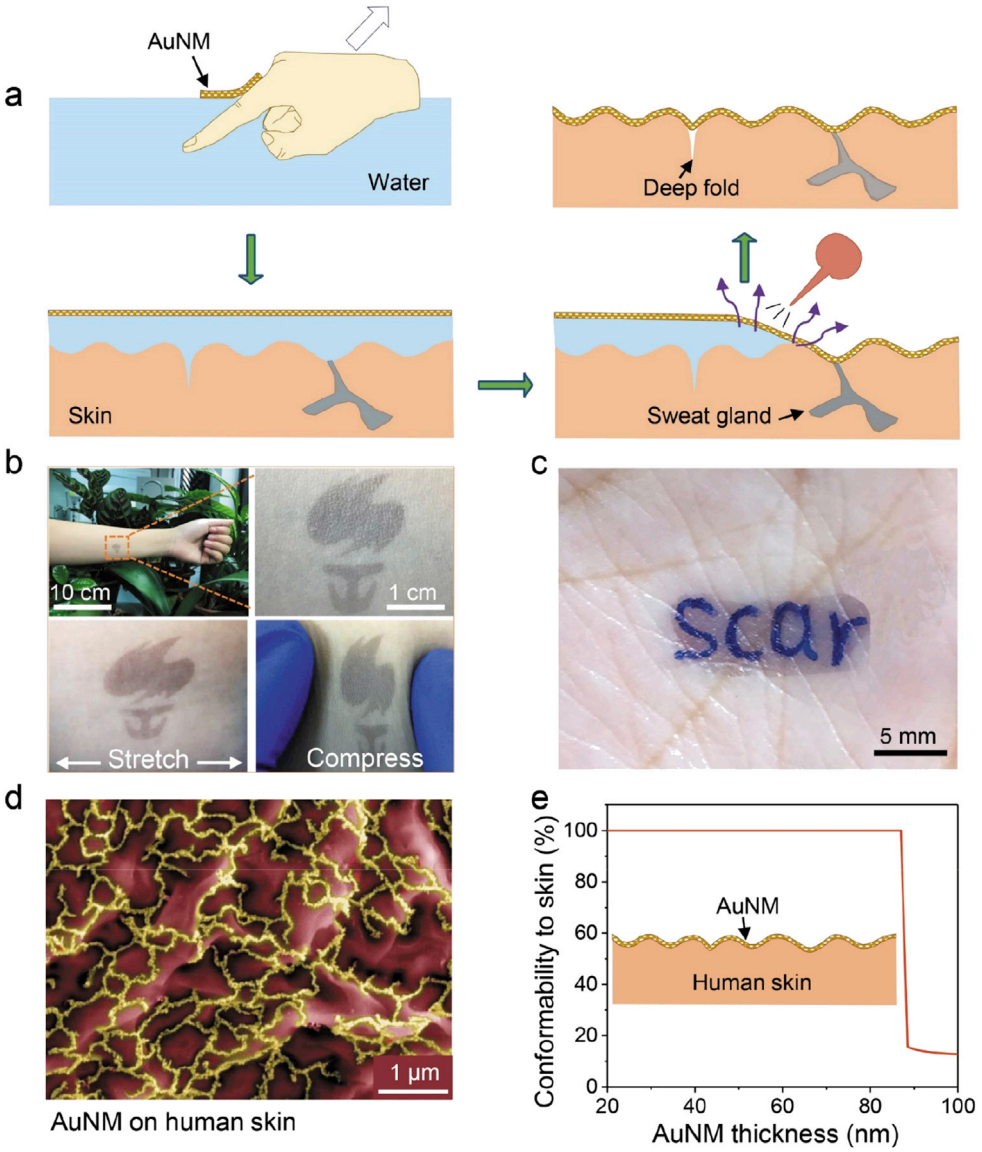

Fig. 1. Transfer, flexibility, transparency, and conformability of the AuNM on skin. (a) Schematic illustration of the fabrication of the AuNM as an epidermal electrode. (b) Patterned AuNM epidermal electrodes on human skin, and the AuNM can be stretched and compressed along with skin textures. (c) The AuNM is transparent on human skin; the word 'scar' is written with a marker on the palm and covered by an AuNM. (d) SEM image of an AuNM electrode well accommodating with human skin textures. (e) The relationship between the conformability (the degree of conformability can be characterized as the ratio between the contact zone and the total area) and the AuNM thickness. SEM = scanning electron microscopy; AuNM = Au nanomesh.

Table 1
Mechanical parameters of the AuNM-human skin system.

Description	Value	Reference
Au-skin adhesion (γ)	18 mJ/m^2	[28]
Plane strain modulus of human skin ($\overline{E}_s$)	130 kPa	[29]
Human skin roughness: wavelength (λ_0)	150 μm	[11]
Human skin roughness: amplitude (h_0)	30 μm	[30]
Plane strain modulus of Au ($\overline{E}_m$)	85.7 GPa	

AuNM = Au nanomesh.

given droplet on a substrate, the volume of the spherical cap is $V = \frac{\pi r^3}{3}(1-\cos\theta)^2(2+\cos\theta)$, and the surface area can be expressed as $S = 2\pi r^2(1-\cos\theta)$, where r is the spherical radius of the water drop and θ is the initial water contact angle. As per the linear relationship between the evaporation rate and surface area, we figured out the relationship between the normalized evaporation rate (v) and the initial water contact angle (θ) to be $v \propto S = k(1-\cos\theta)^{-\frac{1}{3}}(2+\cos\theta)^{-\frac{2}{3}}$ (where k is a factor related to the drop volume V). The normalized water evaporation rate of the drop as a function of contact angle is shown in Fig. 2f. Suppose that two water drops with the same volume are placed on substrates with contact angles of 75° and 10°, respectively, the ratio between their evaporation rates is figured out to be 3.03, which approaches to our experimental result of 3.6. Therefore, the hydrophilic treatment of the AuNM can dramatically improve the sweat evaporation rate when it is placed on skin.

The improved sweat breathability is of great significance for epidermal electronics. Poor sweat breathability of epidermal electronics will lead to redness, itchiness, or even festering of the human skin. Epidermal electronic devices often use an elastomeric or plastic substrate with poor breathability [13,15,21,22]. Although very recently some elastomer films with a water vapor evaporation rate of ~125 g m^{-2} h^{-1} have been developed [12], this value is still

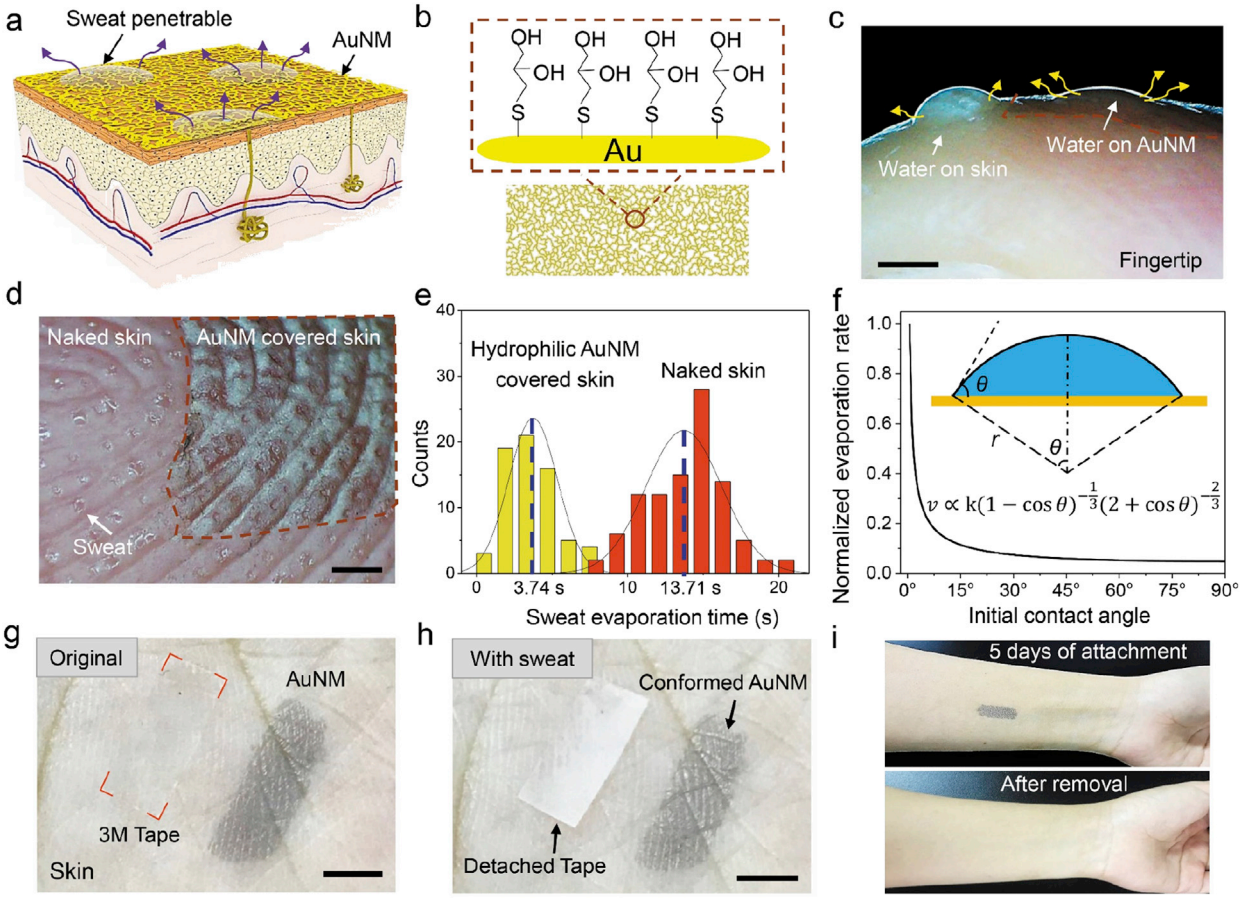

Fig. 2. Sweat breathability of the AuNM on skin. (a) Sweat is penetrable to a mesh-like structure. (b) The AuNM surface was modified to be highly hydrophilic by treated with a monolayer of 1-thioglycerol molecules. (c) Water droplets on naked skin and treated-AuNM-covered skin, showing significantly different wettability. (d) Sweat evaporation on naked skin and hydrophilically treated AuNM-covered skin. (e) Statistical data of the sweat evaporation time for naked skin and hydrophilically treated AuNM-covered skin, showing that the sweat evaporation rate of the AuNM-skin surface is 3.6 times that of naked skin. (f) Normalized drop evaporation rate as a function of the initial contact angle. (g) 3M tape and treated AuNM attached to the skin. (h) After a few sweat cycles, the 3M tape detaches, whereas the AuNM still fully adheres to skin. (i) No redness appeared on skin after 5 D wearing of the hydrophilically treated AuNM. Scale bars are 5 mm. AuNM = Au nanomesh.

far smaller than the maximum daily sweat rate for adults of 600–900 g m^{-2} h^{-1} [35]. Moreover, the integration of functional layers on the elastomer layer will further decrease the sweat evaporation rate of epidermal devices and thus limit the potential applications in which a high sweat evaporation rate is needed. In this work, the sweat evaporation rate of the AuNM-skin surface is almost four times that of naked skin, indicating that the AuNM can be attached for a long term on skin. The effect of the high sweat evaporation rate of the AuNM can be verified by comparing with a piece of breathable tape under a sweating condition. When a blanket 3M tape and a surface-treated AuNM were placed on a dried human palm, both attached well on human skin (Fig. 2g). However, after 10 min of sweating, the 3M tape, although being widely used as a breathable substrate on skin, detached. By contrast, the AuNM was still fully conformable with skin textures, as shown in Fig. 2h.

Surface treatment significantly improves sweat breathability, and it does not cause adverse effects on either electrical property or biosafety to the skin. Electrical resistance of the hydrophilically treated AuNM is stable: a sample attached on skin keeps the resistance almost unchanged (~200 Ω) after 6 cycles of repeated sweating and with sweat evaporation lasting for 6 h (Fig. S7). The on-skin AuNM also exhibits high water resistance, evidenced by the fact that no significant change in resistance of the mesh was found after immersing in water for 40 min, followed by washing with running water for 2 min (Fig. S8). For biosafety, Au is a material with excellent biocompatibility, and after assembling with the 1-thioglycerol monolayer, the AuNM still does not cause skin irritation. Fig. 2i shows that no redness is found in the surface-treated AuNM-covered skin area after 5 days of lamination. The results indicate that the AuNM can be safely and stably attached to the skin without performance degradation.

2.3. Epidermal strain sensor and thermotherapy electrode

The resistance of the AuNM changes along with the skin deformation, and thus, the mesh can be used as an epidermal strain sensor. A piece of AuNM-based strain sensor (size: 16 mm × 8 mm) attached on a finger joint exhibits a relative resistance increase of ~1.5% on finger bending to ~45°, and the resistance decreases to the original value on releasing. The sensing signal of finger motion is pretty stable: the normalized change in resistance is relatively stable, with only a small drift (<1.5%) after 3000 bending cycles (Fig. 3a), and the difference between each of the two adjacent peaks (or valleys) is negligible as per our statistical analysis (Fig. S9).

Such an AuNM is also capable of monitoring the directional motion or rotation of joints. As the wrist rotates, the AuNM (size: 12 mm × 4 mm) attached on the backside of the wrist demonstrates a characteristic change in resistance for each cycle, as shown in Fig. 3b. As the wrist rotates clockwise or anticlockwise, the

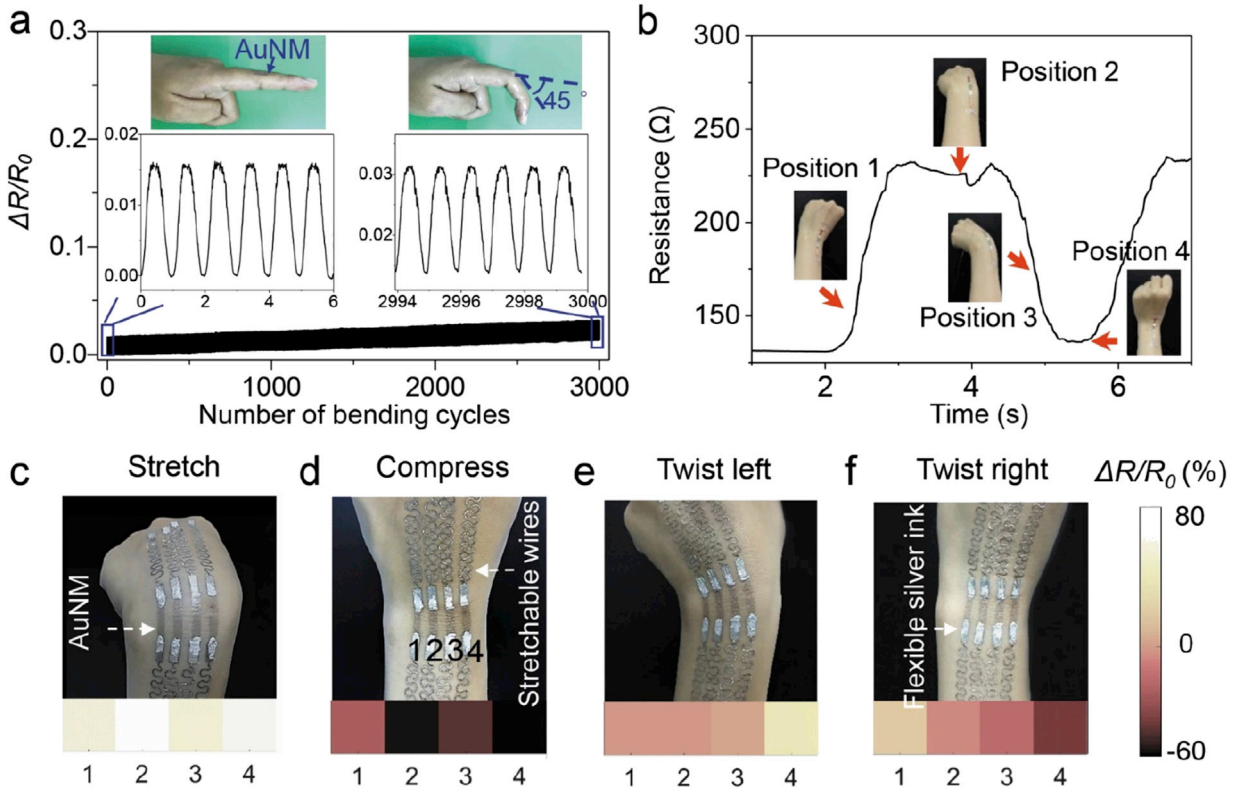

Fig. 3. AuNMs for sensing of skin strain. (a) Normalized change in resistance of the AuNM (size: 16 mm × 8 mm) over 3000 cycles of finger bending and relaxing. (b) The characteristic response of resistance as wrist rotates. (c–f) Detection of strain distributions in four mechanical modes including (c) stretching (corresponding strain of 17.9% ~ 28.6%), (d) compression (strain of −28.6% ~ −21.4%), (e) twisting left (strain of −7.1% ~ 14.3%), and (f) twisting right (strain of −28.6% ~ 7.1%). The AuNM ribbons are labeled as sensor no. 1 to 4. AuNM = Au nanomesh.

resistance always increases at the stretching state and decreases at the compression state (Fig. S10), with a small characteristic valley as the wrist bends forward. The signals well reflect the strain status in the AuNM ribbons (Movie S3). Such a characteristic waveform of the signal is quite useful in human motion recording and recognition and may be extended to the motion pattern recognition of other joints by means of data analysis.

Supplementary video related to this article can be found at https://doi.org/10.1016/j.mtphys.2020.100191.

By applying an array of AuNM ribbons, we were able to distinguish the strain state of different positions of the skin. Mechanical modes of stretching, compressing, and twisting to different directions (Fig. 3c–f) were applied to an array of four parallel AuNM ribbons attached on a wrist, and the resistances were recorded accordingly. The resistance for each ribbon increases when the wrist is stretched, but the changes in resistance differ for the four ribbons, and the differences are reasonably attributed to the non-homogeneous strain distribution of the skin. By contrast, compression caused by bending back will cause a decrease in resistance of the ribbons, and still, the amplitude of the resistance of the four ribbons is not exactly equivalent. Such a non-homogenous distribution of the resistance change, however, does not make any difficulties to judge the bending direction of the wrist: when bending forward, the changes in resistance ($\Delta R/R_0$, where R_0 is the original resistance) of all ribbons are positive; when bending back, $\Delta R/R_0$ of all ribbons are negative. When twisting left, $\Delta R/R_0$ are from negative to positive for the AuNM ribbons from left to right, and the signal is inversed when twisting right. Our result demonstrates that the array of AuNM ribbons could be applied to measure the strain distribution of the skin, as well as to identify the bending direction of joints or hands. In addition, a Bluetooth circuit has been used for epidermal strain sensing on the skin, confirming that our material has a great possibility of application in portable electronics (Fig. S11 and Movie S4).

Supplementary video related to this article can be found at https://doi.org/10.1016/j.mtphys.2020.100191.

Flexible electrodes have been applied for generating Joule heat as a transparent heater or for fabrics under low voltages [36,37]. The AuNM studied here, as a conformable, biocompatible, highly breathable, and high conducting material (40–60 Ω sq.$^{-1}$ on skin textures), is an ideal heater for epidermal thermotherapy. Fig. S12a shows a patterned AuNM heater on a skin replica. By applying a small voltage that is safe to the human body, the AuNM will generate well-controlled Joule heat. In particular, from the relationship between the temperature (T) and the working voltage (Fig. S12b), the working temperature of the epidermal heater follows the relationship $\Delta T \propto U^2/R$ (where U is the applied direct current voltage). Thus, the thermotherapy temperature can be precisely controlled by simply controlling the aspect ratio of the AuNM ribbons because it determines the resistance (Fig. S12c). In addition, the elevation of the temperature of the heater is fast: the temperature sharply increases and achieves a stable value within 10 s owing to the small heat capacity of the nanoscale mesh. Such a flexible, conformable, and sweat-permeable epidermal electrode can generate a suitable temperature (40–60 °C) and infrared irradiation with a wavelength centered at ~8 μm, which are desired for moxibustion thermotherapy with rapid heating and precise temperature control. By contrast, conventional moxa-moxibustion by burning moxa sticks cannot control the temperature well, such that it may hurt the skin and will also cause

pollution to the air. Moreover, this tattoo-like AuNM can offer high comfort because the mesh feels imperceptible on the skin.

2.4. Sensing mechanism of the AuNM electrode

The sensing capability of the AuNM is due to distributed rupture on stretching and fast cold welding of ruptured Au nanowires when relaxed. During stretching, cracks are generated along the deep folds, as a result of the huge local area mismatch between the skin and the AuNM (Fig. 4a); thus, resistance increases accordingly. The cracks, however, can be partly or fully recovered on release or compression (Fig. 4b), and the corresponding resistance of the mesh recovers. Aside from the local rupture and recovery along with the deep folds, delocalized rupture and self-healing over the whole mesh will also contribute to sensing (especially when the strain is large). From the *in situ* atomic force microscopy (AFM) images (Fig. 4c and d), an AuNM on a flat elastomer surface forms highly distributed tiny cracks under stretching, and on release, such cracks rapidly disappear. This process will also cause significant resistance increase and recovery. The recovery of the AuNM lies in the fast cold welding of nanoscale gold nanowires when they are contacted [38,39]. The rupture and recovery are found to be

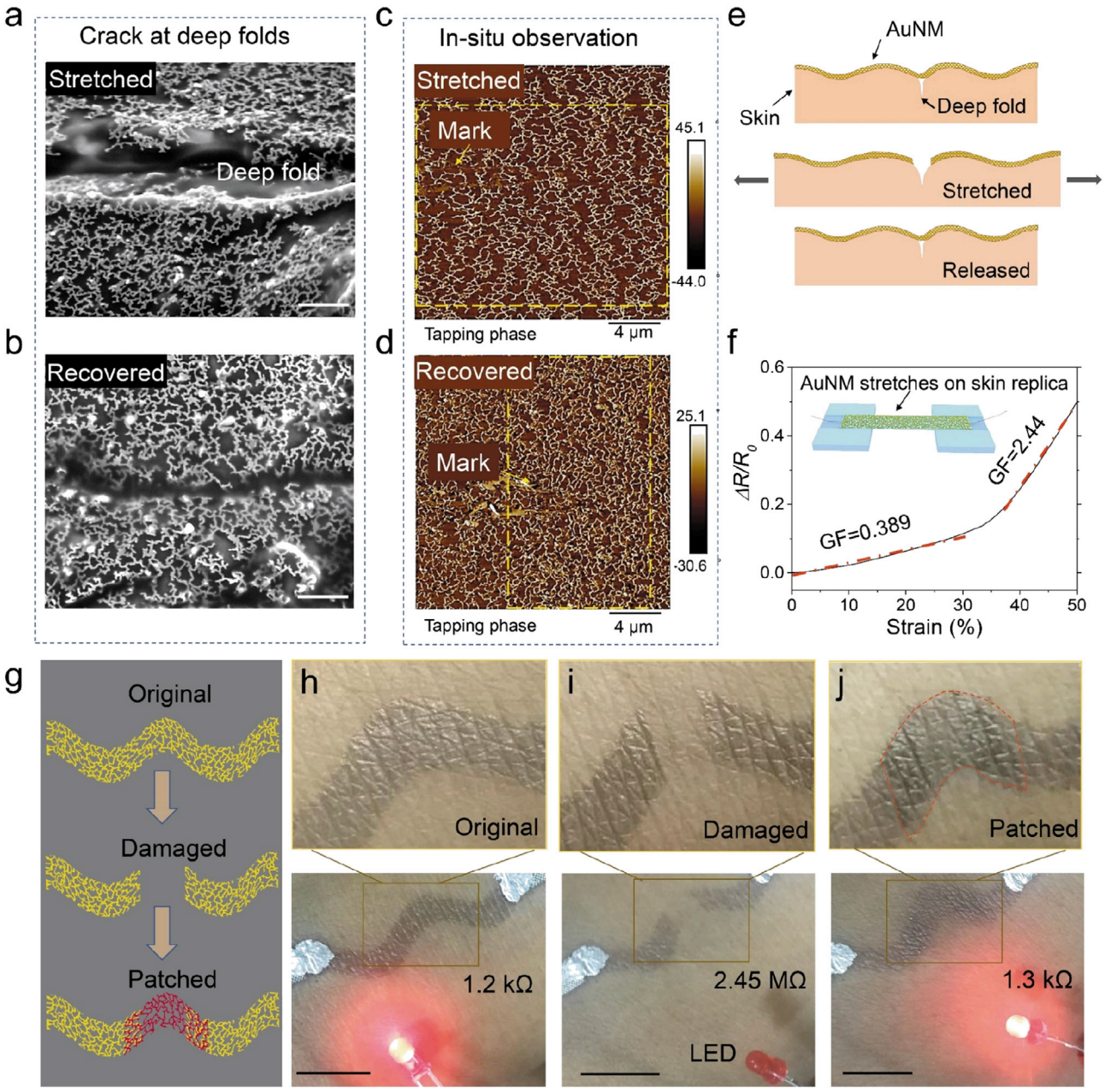

Fig. 4. Sensing mechanism of the AuNM on skin. (a) Cracks generated in the deep textured areas on stretching. (b) Recovery of the cracks after releasing. Scale bars are 1 μm. (c–d) The in situ recovery of the cracks after releasing. The dashed rectangles in panels (c) and (d) represent the same area. (e) Schematic of the conformability of the AuNM on skin, showing that the AuNM can comply well with convex skin texture but form cracks along deep folds owing to huge area mismatch. (f) The resistance change as a function of strain of the AuNM on PDMS with skin texture. (g) Schematic of the reparable epidermal electrode. (h) A patterned AuNM epidermal electrode with a resistance of 1.2 kΩ. (i) After damage, the AuNM becomes non-conducting. (j) An extra AuNM patch repairs the electrical connection of the damaged AuNM, and resistance recovers to 1.3 kΩ. Scale bars are 1 cm. LED = light-emitting diode; AuNM = Au nanomesh; PDMS = polydimethylsiloxane.

reversible, and this well explains the high stability of the sensing performance. The detailed sensing mechanism is clearly illustrated in the schematics of Fig. 4e. The sensitivity to the strain (ε) can be characterized using a parameter gauge factor (*GF*, defined as $GF = \delta\left(\frac{\Delta R}{R_0}\right) \Big/ \delta\varepsilon$). Our measured resistance-strain curve indicates that the resistance of the mesh increases with increasing strain, leading to a *GF* of 0.389 when the strain is lower than 30% and 2.44 as strain increases to higher than 40% (Fig. 4f).

The high stretchable AuNM can deform along with human skin, but it is easily damaged by scratching because of the poor adhesion between gold and human skin, leading to a connection failure. The damage, however, can be fixed by attaching a piece of extra AuNM ribbon, similar to the overlay alignment in photolithography (Fig. 4g). The process is confirmed by deliberately scratching an AuNM ribbon on the skin to cause damage to an AuNM circuit (original resistance, R ~1.2 kΩ) connected to a light-emitting diode (LED) bulb (Fig. 4h). After damage, the measured resistance changes to 2.45 MΩ, corresponding to the impedance of human skin. Accordingly, the LED bulb interconnected to the mesh is off (Fig. 4i). Next, an extra piece of AuNM is patched directly to the damaged area, the resistance recovers to 1.3 kΩ, and the LED is on again (Fig. 4j). The fixed AuNM circuit on the skin can still maintain its high flexibility (Movie S5) without a significant difference with the original AuNM. The repairability of the on-skin AuNM is reasonably attributed to the cold welding of nanoscale Au nanowires [39].

Supplementary video related to this article can be found at https://doi.org/10.1016/j.mtphys.2020.100191.

2.5. Comparison with other epidermal electrodes

The AuNM presents superior overall performances compared with existing on-skin electrodes. First, the mesh structure with serpentine Au ligaments allows the AuNM to stretch greatly, to be highly transparent to light, and to be highly conducting as well. Our experimental results show that the AuNM presents a sheet resistance comparable with that of commercial indium tin oxide films. It can be stretched to strains higher than 100%, in combination with a transparency higher than 80%. By contrast, the Au nanotrough network electrode reported by Miyamoto et al. [23], although being an excellent selection as an epidermal electrode and sensor, was not transparent and could not be significantly stretched if no pre-strain is applied because the Au nanostructures are straight. Another epidermal electrode the graphene electronic tattoo [13] is transparent; its electrical conductivity and stretchability (can be achieved by fabricating an open mesh), however, are limited compared with our AuNMs. In addition, the fast cold welding effect of the nanoscale Au wires in our AuNMs plays a subtle role in sensing, giving rise to a more stable signal over 3000 cycles of finger bending and the ability to identify joint rotation direction and strain mapping of the skin.

Second, the AuNM electrodes are superior in sweat breathability. Sweating affects not only the heat balance but also the tactile system of skin. It is known that discomfort of skin is significant in areas of perspiration, and some chemicals and biological toxic substances are much more harmful to skin in the hot and wet environment [40]. The reason is that sweat provides a hot and humid environment for bacterial growth, which causes undesired results, such as body odor and irritation [41–43]. Although some other on-skin electronic materials are also breathable, their breathability, however, is poorer than that of naked skin. As a result, they might not be applied under conditions of hot weather or during strenuous exercises, during which heavy sweating often happens. For example, graphene electrodes, although being extremely thin, still have an adverse effect on sweat breathability. By contrast, the hydrophilically treated AuNM studied here could significantly improve the wettability and thereby enhance the sweat evaporation rate to a value a few times higher than that of the naked skin. Such a high sweat breathability of our sensors is quite important for long-term and comfortable attachment on the skin.

Third, the AuNM can be healed rapidly. Some electronic materials are self-healable based on reconstructing the inherent reversible chemical bonds between the cracking interfaces [37,44,45]. However, this manner of healing needs a long time for chemical bonds to reconstruct. Here, we use a piece of new AuNM to patch directly onto the damaged area for repairing, and the AuNM epidermal electrodes can recover their functions immediately, thus enhancing the reliability of the AuNM.

3. Conclusions

In summary, we have demonstrated substrate-free, highly breathable, and reparable AuNMs for epidermal electronics. By applying a hydrophilic treatment, the on-skin AuNM presents high wettability that improves the sweat evaporation rate of the skin by a factor of 3.6. The high sweat breathability is of great significance to conformability and long-term attachment. The AuNM also presents high sensing performance to skin strain caused by joint motion: it is capable of mapping skin strains, sensing mechanical modes of stretching, compression, and joint twisting and identifying joint rotation directions. The sensing performance is exceptionally stable: the signal remains stable after 3000 bending/releasing cycles, with only a small drift of 1.5%. The sensing capability lies in the local cracking and fast cold welding of nanoscale Au nanowires on straining and relaxing, respectively. The fast cold welding also enables the repairment of the damaged AuNM by directly attaching a new AuNM patch onto the damaged area. Furthermore, the high conformability of the AuNM allows for promising applications in epidermal signal collection and thermotherapy. The method of surface treatment to enhance the sweat breathability of epidermal electronics (even superior to that of naked skin) may also be extended to other electronic materials.

4. Experimental section

4.1. The hydrophilic treatment of the AuNM

1-thioglycerol (Macklin, 95 wt%) was dissolved in water at a volume ratio of 1:5 (1-thioglycerol:water). By adding 1-thioglycerol solution to water with the floating AuNM, the metal surface assembled a monolayer of 1-thioglycerol molecules by forming a strong Au–S bond.

4.2. The statistics of evaporation time for the sweat droplets

A piece of hydrophilically treated AuNM transferred onto a sweaty palm was observed under an optical microscope by capturing some videos of sweat cycles. From the videos, 168 sweating droplets were taken as the research samples, and the evaporation times of each sweat droplet in the naked skin area and AuNM-covered area were calculated and analyzed from the videos.

4.3. Repairment of the damaged AuNM

After the AuNM electrode was damaged intentionally, an adhesive tape mask patterned by laser cutting was put upside down on the human skin aligning the previous AuNM ribbon. Then, a piece of new AuNM was transferred onto the human skin from water, and the AuNM ribbon patch was repaired after removing the mask.

4.4. Material characterization

The tape masks for patterning the AuNM were cut by using a CO_2 laser cutting machine (WE-640, Xiamen Waner). The SEM images were taken by using a TESCAN scanning electron microscope. The transmittance of the samples was recorded using a PerkinElmer Lambda 950 spectrometer. The weight loss of water or permeability was measured using an electronic analytical balance. The electrical resistance of the AuNM was measured by using a multimeter (Keithley 2100). The bending of the artificial finger was carried out using a custom-made stretching machine, and a cyclic test was carried out after a few cycles of finger bends to get stable data. The infrared thermal response was tested using a thermal infrared imager (FLIR, C3). The sweat evaporation rate was measured at a temperature of ~20 °C and a humidity of ~75%. The AFM images were taken by using an atomic force microscope (AFM Bruker Dimension Edge). Subjects of on-skin measurements were all authors. The on-skin experiment protocol was reviewed and approved by the committee of the Institutional Review Board of SUSTech.

4.5. Experiments on human subjects

On-skin experiments were conducted under the approval from the Institutional Review Board at the Southern University of Science and Technology (protocol number: 20190007).

Author contributions

C.F.G. conceived the idea. Y.W. and T.H. conducted the experiments, L.W. and N.L. carried out the calculation. The manuscript was written with the contributions of all authors. All authors have given approval to the final version of the manuscript.

Declaration of competing interest

The authors declare that they have no known competing financial interests or personal relationships that could have appeared to influence the work reported in this paper.

Acknowledgments

The authors acknowledge the financial support of the National Natural Science Foundation of China (51771089, U1613204), the 'Guangdong Innovative and Entrepreneurial Research Team Program' under contract 2016ZT06G587, the 'Science Technology and Innovation Committee of Shenzhen Municipality' (JCYJ20160613160524999), and the 'Shenzhen Sci-Tech Fund' (KYTDPT20181011104007). The authors would like to thank the Materials Characterization and Preparation Center, Southern University of Science and Technology, for providing apparatuses for the preparation of the Au nanomeshes.

Appendix A. Supplementary data

Supplementary data to this article can be found online at https://doi.org/10.1016/j.mtphys.2020.100191.

References

[1] B. Chu, W. Burnett, J.W. Chung, Z. Bao, Bring on the bodyNET, Nat. News 549 (2017) 328–330, https://doi.org/10.1038/549328a.
[2] D.-H. Kim, N. Lu, R. Ma, Y.-S. Kim, R.-H. Kim, S. Wang, J. Wu, S.M. Won, H. Tao, A. Islam, K.J. Yu, T.-i. Kim, T. Chowdhury, M. Ying, L. Xu, M. Li, H.-J. Chung, H. Keum, M. McCormick, P. Liu, Y.-W. Zhang, F.G. Omenetto, Y. Huang, T. Coleman, J.A. Rogers, Epidermal electronics, Science 333 (2011) 838–843, https://doi.org/10.1126/science.1206157.
[3] N. Lu, D.-H. Kim, Flexible and stretchable electronics paving the way for soft robotics, Soft Robot. 1 (2014) 53–62, https://doi.org/10.1089/soro.2013.0005.
[4] M. Ha, S. Lim, S. Cho, Y. Lee, S. Na, C. Baig, H. Ko, Skin-inspired hierarchical polymer architectures with gradient stiffness for spacer-free, ultrathin, and highly sensitive triboelectric sensors, ACS Nano 12 (2018) 3964–3974, https://doi.org/10.1021/acsnano.8b01557.
[5] Y. Wan, Y. Wang, C.F. Guo, Recent progresses on flexible tactile sensors, Mater. Today Phys. 1 (2017) 61–73, https://doi.org/10.1016/j.mtphys.2017.06.002.
[6] A. Chortos, J. Liu, Z. Bao, Pursuing prosthetic electronic skin, Nat. Mater. 15 (2016) 937–950, https://doi.org/10.1038/nmat4671.
[7] S. Xu, A. Jayaraman, J.A. Rogers, Skin sensors are the future of health care, Nature 571 (2019), https://doi.org/10.1038/d41586-019-02143-0, 391-321.
[8] D.-H. Kim, J. Viventi, J.J. Amsden, J. Xiao, L. Vigeland, Y.-S. Kim, J.A. Blanco, B. Panilaitis, E.S. Frechette, D. Contreras, D.L. Kaplan, F.G. Omenetto, Y. Huang, K.-C. Hwang, M.R. Zakin, B. Litt, J.A. Rogers, Dissolvable films of silk fibroin for ultrathin conformal bio-integrated electronics, Nat. Mater. 9 (2010) 511–517, https://doi.org/10.1038/NMAT2745.
[9] Y. Chen, S. Lu, S. Zhang, Y. Li, Z. Qu, Y. Chen, B. Lu, X. Wang, X. Feng, Skin-like biosensor system via electrochemical channels for noninvasive blood glucose monitoring, Sci. Adv. 3 (2017), https://doi.org/10.1126/sciadv.1701629 e1701629.
[10] H. Lee, C. Song, Y.S. Hong, M.S. Kim, H.R. Cho, T. Kang, K. Shin, S.H. Choi, T. Hyeon, D.-H. Kim, Wearable/disposable sweat-based glucose monitoring device with multistage transdermal drug delivery module, Sci. Adv. 3 (2017), https://doi.org/10.1126/sciadv.1601314 e1601314.
[11] J.W. Jeong, W.-H. Yeo, A. Akhtar, J.J.S. Norton, Y.-J. Kwack, S. Li, S.-Y. Jung, Y. Su, W. Lee, J. Xia, H. Cheng, Y. Huang, W.-S. Choi, T. Bretl, J.A. Rogers, Materials and optimized designs for human-machine interfaces via epidermal electronics, Adv. Mater. 25 (2013) 6839–6846, https://doi.org/10.1002/adma.201301921.
[12] Y. Wang, Y. Qiu, S.K. Ameri, H. Jang, Z. Dai, Y. Huang, N. Lu, Low-cost, μm-thick, tape-free electronic tattoo sensors with minimized motion and sweat artifacts, npj Flexible Electron 2 (2018) 6, https://doi.org/10.1038/s41528-017-0019-4.
[13] S.K. Ameri, R. Ho, H. Jang, L. Tao, Y. Wang, L. Wang, D.M. Schnyer, D. Akinwande, N. Lu, Graphene electronic tattoo sensors, ACS Nano 11 (2017) 7634–7641, https://doi.org/10.1021/acsnano.7b02182.
[14] L. Wang, S. Qiao, S.K. Ameri, H. Jeong, N. Lu, A thin elastic membrane conformed to a soft and rough substrate subjected to stretching/compression, J. Appl. Mech. 84 (2017) 111003, https://doi.org/10.1115/1.4037740.
[15] J.-H. Kim, S.-R. Kim, H.-J. Kil, Y.-C. Kim, J.-W. Park, Highly conformable, transparent electrodes for epidermal electronics, Nano Lett. 18 (2018) 4531–4540, https://doi.org/10.1021/acs.nanolett.8b01743.
[16] J. Lee, S. Shin, S. Lee, J. Song, S. Kang, H. Han, S. Kim, S. Kim, J. Seo, D. Kim, T. Lee, Highly sensitive multifilament fiber strain sensors with ultrabroad sensing range for textile electronics, ACS Nano 12 (2018) 4259–4268, https://doi.org/10.1021/acsnano.8b05295.
[17] M. Isik, T. Lonjaret, H. Sardon, R. Marcilla, T. Herve, G.G. Mallirars, E. Ismailova, D. Mecerreyes, Cholinium-based ion gels as solid electrolytes for long-term cutaneous electrophysiology, J. Mater. Chem. C 3 (2015) 8942–8948, https://doi.org/10.1039/c5tc01888a.
[18] J.J. Norton, D.S. Lee, J.W. Lee, W. Lee, O. Kwon, P. Won, S.-Y. Jung, H. Cheng, J.-W. Jeong, A. Akce, S. Umunna, I. Na, Y.H. Kwon, X.-Q. Wang, Z. liu, U. Paik, Y. Huang, T. Bretl, W.-H. Yeo, J.A. Rogers, Soft, curved electrode systems capable of integration on the auricle as a persistent brain–computer interface, Proc. Natl. Acad. Sci. Unit. States Am. 112 (2015) 201424875, https://doi.org/10.1073/pnas.1424875112.
[19] J.Y. Sun, C. Keplinger, G.M. Whitesides, Z. Suo, Ionic skin, Adv. Mater. 26 (2014) 7608–7614, https://doi.org/10.1002/adma.201403441.
[20] *https://www.wacker.com.*
[21] K.-I. Jang, S.H. Han, S. Xu, K.E. Mathewson, Y. Zhang, J.-W. Jeong, G.-T. Kim, R.C. Webb, J.w. Lee, T.J. Dawidczyk, R.H. Kim, Y.M. Song, W.-H. Yeo, S. Kim, H. Cheng, S.I. Rhee, J. Chung, B. Kim, H.U. Chung, D. Lee, Y. Yang, M. Cho, J.G. Gaspar, R. Carbonari, M. Fabiani, G. Gratton, Y. Huang, J.A. Rogers, Rugged and breathable forms of stretchable electronics with adherent composite substrates for transcutaneous monitoring, Nat. Commun. 5 (2014) 4779, https://doi.org/10.1038/ncomms5779.
[22] Y. Chen, B. Lu, Y. Chen, X. Feng, Breathable and stretchable temperature sensors inspired by skin, Sci. Rep. 5 (2015) 11505, https://doi.org/10.1038/srep11505.
[23] A. Miyamoto, S. Lee, N.F. Cooray, S. Lee, M. Mori, N. Matsuhisa, H. Jin, L. Yoda, T. Yokota, A. Itoh, M. Sekino, H. Kawasaki, T. Ebihara, M. Amagai, T. Someya, Inflammation-free, gas-permeable, lightweight, stretchable on-skin electronics with nanomeshes, Nat. Nanotechnol. 12 (2017) 907–913, https://doi.org/10.1038/NNANO.2017.125.
[24] C.F. Guo, T. Sun, Q. Liu, Z. Suo, Z. Ren, Highly stretchable and transparent nanomesh electrodes made by grain boundary lithography, Nat. Commun. 5 (2014) 3121, https://doi.org/10.1038/ncomms4121.
[25] D.S. Gray, J. Tien, C.S. Chen, High-conductivity elastomeric electronics, Adv. Mater. 16 (2004) 393–397, https://doi.org/10.1002/adma.200306107.
[26] T.C. Shyu, P.F. Damasceno, P.M. Dodd, A. Lamoureux, L. Xu, M. Shlian, M. Shtei, S.C. Glotzer, N.A. Kotov, A kirigami approach to engineering elasticity in nanocomposites through patterned defects, Nat. Mater. 14 (2015) 785, https://doi.org/10.1038/NMAT4327.

[27] L. Wang, N. Lu, Conformability of a thin elastic membrane laminated on a soft substrate with slightly wavy surface, J. Appl. Mech. 83 (2016), https://doi.org/10.1115/1.4032466, 041007.
[28] C.J. Brennan, J. Nguyen, E.T. Yu, N. Lu, Interface adhesion between 2D materials and elastomers measured by buckle delaminations, Adv. Mater. Inter. 2 (2015) 1500176, https://doi.org/10.1002/admi.201500176.
[29] C. Pailler-Mattei, S. Bec, H. Zahouani, In vivo measurements of the elastic mechanical properties of human skin by indentation tests, Med. Eng. Phys. 30 (2008) 599, https://doi.org/10.1016/j.medengphy.2007.06.011.
[30] L. Tchvialeva, H. Zeng, I. Markhvida, D.I. McLean, H. Lui, T.K. Lee, Skin roughness assessment in new developments in biomedical engineering, in: D. Campolo (Ed.), InTech, Vukovar, Croatia, 2010, pp. 341–358. Ch. 18.
[31] G. Dunn, S. Wilson, B. Duffy, K. Sefiane, Evaporation of a thin droplet on a thin substrate with a high thermal resistance, Phys. Fluids 21 (2009), https://doi.org/10.1063/1.3121214, 052101.
[32] S.M. Rowan, M.I. Newton, G. Mchale, Evaporation of microdroplets and the wetting of solid surfaces, J. Phys. Chem. 99 (1995) 13268–13271, https://doi.org/10.1021/j100035a034.
[33] R.G. Picknett, R. Bexon, Evaporation of sessile or pendant drops in still air, J. Colloid Interface Sci. 61 (1977) 336–350, https://doi.org/10.1016/0021-9797(77)90396-4.
[34] K. Birdi, D. Vu, A. Winter, A study of the evaporation rates of small water drops placed on a solid surface, J. Phys. Chem. 93 (1989) 3702–3703, https://doi.org/10.1021/j100346a065.
[35] G.W. Mack, E.R. Nadel, Body fluid balance during heat stress in humans, Environ. Physiol. (1996) 187–214, https://doi.org/10.1002/cphy.cp040110.
[36] L. Cai, A.Y. Song, P. Wu, P.-C. Hsu, Y. Peng, J. Chen, C. Liu, P.B. Catrysse, Y. Liu, A. Yang, C. Zhou, C. Zhou, S. Fan, Y. Cui, Warming up human body by nanoporous metallized polyethylene textile, Nat. Commun. 8 (2017) 496, https://doi.org/10.1038/s41467-017-00614-4.
[37] A.M. Hussain, E.B. Lizardo, G.A. Torres Sevilla, J.M. Nassar, M.M. Hussain, Ultrastretchable and flexible copper interconnect-based smart patch for adaptive thermotherapy, Adv. Healthc. Mater. 4 (2015) 665–673, https://doi.org/10.1002/adhm.201400647.
[38] C.F. Guo, Q. Liu, G. Wang, Y. Wang, Z. Shi, Z. Suo, C.-W. Chu, Z. Ren, Fatigue-free, superstretchable, transparent, and biocompatible metal electrodes, Proc. Natl. Acad. Sci. U.S.A. 112 (2015) 12332–12337, https://doi.org/10.1073/pnas.1516873112.
[39] C.F. Guo, Y. Lan, T. Sun, Z. Ren, Deformation-induced cold-welding for self-healing of super-durable flexible transparent electrodes, Nanomater. Energy 8 (2014) 110–117, https://doi.org/10.1016/j.nanoen.2014.05.011.
[40] D.G. Rainham, K.E. Smoyer-Tomic, The role of air pollution in the relationship between a heat stress index and human mortality in Toronto, Environ. Res. 93 (2003) 9–19, https://doi.org/10.1016/S0013-9351(03)00060-4.
[41] B. Usher, Human sweat as a culture medium for bacteria: a preliminary report, Arch. Dermatol. Syphilol. 18 (1928) 276–280, https://doi.org/10.1001/archderm.1928.02380140100009.
[42] E.A. Grice, J.A. Segre, The skin microbiome, Nat. Rev. Microbiol. 9 (2011) 244–253, https://doi.org/10.1038/nrmicro2537.
[43] L. Teufel, A. Pipal, K.C. Schuster, T. Staudinger, B. Redl, Material-dependent growth of human skin bacteria on textiles investigated using challenge tests and DNA genotyping, J. Appl. Microbiol. 108 (2010) 450–461, https://doi.org/10.1111/j.1365-2672.2009.04434.x.
[44] T. Wang, Y. Zhang, Q. Liu, W. Cheng, X. Wang, L. Pan, B. Xu, H. Xu, A self-healable, highly stretchable, and solution processable conductive polymer composite for ultrasensitive strain and pressure sensing, Adv. Funct. Mater. 28 (2018) 1705551, https://doi.org/10.1002/adfm.201705551.
[45] Y. Huang, M. Zhong, Y. Huang, M. Zhu, Z. Pei, Z. Wang, Q. Xue, X. Xie, C. Zhi, A self-healable and highly stretchable supercapacitor based on a dual cross-linked polyelectrolyte, Nat. Commun. 6 (2015) 10310, https://doi.org/10.1038/ncomms10310.